Ga for Zn Cation Exchange Allows for Highly Luminescent and Photostable InZnP-Based Quantum Dots

Pietra, Francesca; Kirkwood, Nick; De Trizio, Luca; Hoekstra, Anne W.; Kleibergen, Lennart; Renaud, Nico; Koole, Rolf; Baesjou, Patrick J.; Manna, Liberato; Houtepen, Arjan

DOI
10.1021/acs.chemmater.7b00848

Publication date
2017

Document Version
Final published version

Published in
Chemistry of Materials

CHEMISTRY OF MATERIALS

Article

pubs.acs.org/cm

Ga for Zn Cation Exchange Allows for Highly Luminescent and Photostable InZnP-Based Quantum Dots

Francesca Pietra,[†,#] Nicholas Kirkwood,[†,#] Luca De Trizio,[‡] Anne W. Hoekstra,[†] Lennart Kleibergen,[†] Nicolas Renaud,[†] Rolf Koole,[∥] Patrick Baesjou,[∥,⊥] Liberato Manna,[‡,§] and Arjan J. Houtepen*[,†]

[†]Optoelectronic Materials Section, Faculty of Applied Sciences, Delft University of Technology, Van der Maasweg 9, 2629 HZ Delft, The Netherlands

[‡]Department of Nanochemistry, Istituto Italiano di Tecnologia (IIT), via Morego, 30, 16163 Genova, Italy

[§]Kavli Institute of Nanoscience, Delft University of Technology, Lorentzweg 1, 2628 CJ Delft, The Netherlands

[∥]Philips Lighting, High Tech Campus 44, 5656 AE Eindhoven, The Netherlands

[⊥]Soft Condensed Matter, Debye Institute, Utrecht University, Princetonplein 5, 3584 CC Utrecht, The Netherlands

Supporting Information

ABSTRACT: In this work, we demonstrate that a preferential Ga-for-Zn cation exchange is responsible for the increase in photoluminescence that is observed when gallium oleate is added to InZnP alloy QDs. By exposing InZnP QDs with varying Zn/In ratios to gallium oleate and monitoring their optical properties, composition, and size, we conclude that Ga^{3+} preferentially replaces Zn^{2+}, leading to the formation of InZnP/InGaP core/graded-shell QDs. This cation exchange reaction results in a large increase of the QD photoluminescence, but only for InZnP QDs with Zn/In ≥ 0.5. For InP QDs that do not contain zinc, Ga is most likely incorporated only on the quantum dot surface, and a PL enhancement is not observed. After further growth of a GaP shell and a lattice-matched ZnSeS outer shell, the cation-exchanged InZnP/InGaP QDs continue to exhibit superior PL QY (over 70%) and stability under long-term illumination (840 h, 5 weeks) compared to InZnP cores with the same shells. These results provide important mechanistic insights into recent improvements in InP-based QDs for luminescent applications.

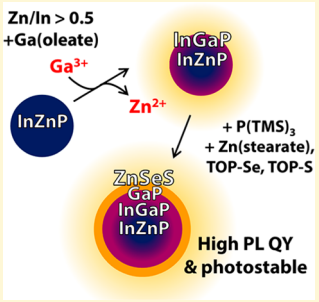

INTRODUCTION

The unique and tunable optical and electrical properties of colloidal quantum dots (QDs) make them promising candidates for application in biological labeling, lighting, displays, solar cells, and sensors.[1−5] Among all semiconductor QDs materials, cadmium chalcogenides have been the most intensively investigated.[4−9] However, the application of these materials is often restricted due to the high toxicity of Cd, necessitating the development of alternative, low-toxicity quantum dot materials. Indium phosphide (InP) is one of the most promising compounds in this context, combining size-tunable emission in the visible and near-infrared spectral range with a low intrinsic toxicity.[10−25] However, in terms of photoluminescence (PL) quantum yield (QY), PL stability, and spectral width of the PL emission peak, InP QDs cannot yet compete with Cd-based systems.

Recently, we have reported the synthesis of InZnP alloy QDs whose structural and optical properties can be tuned by varying the concentration of zinc.[26] For simplicity, we will omit subscripts denoting cation and anion stoichiometry in this work. Varying the concentration of zinc in these QDs allows for the formation of QDs with a tunable lattice constant that, in principle, can match that of a chosen shell material, possibly creating strain-free core/shell heterostructures. By matching the lattice constant of the InZnP core and the ZnSeS shell material, an overall PL QY as high as ∼60% was achieved.[26] The growth of a GaP intermediate layer (or buffer layer) was recently reported by Kim et al. as a means of further increasing the PL QY of indium phosphide based QDs to above 80%.[27,28] Upon addition of Ga^{3+} ions to a reaction mixture containing InZnP alloy QDs, they observed the formation of an outer GaP layer, which was attributed to a cation exchange (CE) reaction between In^{3+} and Ga^{3+} ions. This shell was believed to efficiently passivate surface defects of InP cores, thereby leading to an enhanced PL QY.[8,18,27−29]

Here, we show that the addition of Ga^{3+} ions to a reaction mixture of InZnP QDs increases their PL QY only if the Zn/In ratio in the QD core exceeds 0.5. We study the optical properties, composition, and size of these QDs during the reaction with Ga^{3+}, and our results clearly indicate that a CE reaction takes place preferentially between Ga^{3+} and Zn^{2+} ions, rather than between Ga^{3+} and In^{3+}, leading to a compositionally graded InZnP/InGaP core−shell system. We demonstrate that a careful choice of both the Zn content in the core QDs and the amount of Ga that is subsequently added can be exploited to improve the PL QY of the resulting QDs from 10% up to 50%, which can be increased up to 55% by adding more phosphorus precursor to deliberately grow a GaP-only shell (see Figure 1a).

Received: February 28, 2017
Revised: June 6, 2017
Published: June 6, 2017

DOI: 10.1021/acs.chemmater.7b00848
Chem. Mater. 2017, 29, 5192−5199

Furthermore, we demonstrate that the cation-exchanged InZnP/InGaP QDs continue to exhibit superior photoluminescence properties compared to InZnP QDs following overgrowth of a lattice-matched outer ZnSeS shell (variable Se/S ratio). We report unoptimized PL QYs up to 75% while retaining a narrow emission band (full width at half-maximum of 52 nm), and crucially for phosphor applications, the QDs exhibit photostability during prolonged irradiation with a blue LED. This demonstrates the importance of the Ga-for-Zn cation exchange reaction for commercially relevant applications.

EXPERIMENTAL METHODS

Materials. Indium(III) acetate ($In(OAc)_3$, 99.99%), zinc(II) acetate ($Zn(OAc)_2$, 99.99%), palmitic acid (PA, $C_{15}H_{31}COOH$, 99.99%, stored at −20 °C), gallium(III) chloride (beads, Sigma-Aldrich, 99.99%), tris(trimethylsilyl)-phosphine ($P(TMS)_3$, 95%), 1-octadecene (ODE, 95%), oleic acid (Sigma-Aldrich, 99.99%), ammonium sulfide solution ($(NH_4)_2S$, 20% in H_2O), 1-octadecene (ODE, 95%), formamide (FA, 99%), dimethylformamide (DMF, 99%), Zn stearate (technical grade), sulfur powder (99.98% trace metals basis), and trioctylphosphine (TOP, 90% technical grade) were purchased from Sigma-Aldrich. Selenium powder (99.98% trace metals basis) was purchased by Chem Pure. All the chemicals were used without further purification.

Synthesis of Green and Yellow Emitting InZnP Alloy QDs. InZnP QDs were synthesized following an adaptation of our previously reported method.[26] In a typical synthesis, 35 mg of $In(OAc)_3$ (0.12 mmol), a desired amount of $Zn(OAc)_2$, and 91 mg of palmitic acid (0.36 mmol) were mixed together with 7 mL of 1-octadecene in a three-neck flask. The solution was degassed under vacuum for 2 h at 120 °C. After heating up the reaction mixture to 300 °C under nitrogen flow, 17 μL of $P(TMS)_3$ (0.06 mmol; 15 mg) in 1 mL of ODE was rapidly injected into the flask. The temperature was then lowered to 270 °C, and the QDs were allowed to grow for 2 h. This "hot" crude reaction solution was immediately used for the CE reactions or for the synthesis of red emitting QDs (see below). Alternatively, to collect the InZnP QDs, the reaction flask was rapidly cooled to room temperature and the QDs were washed three times by dispersion in toluene, followed by precipitation by addition of a mixture of ethanol:acetone (1:3), and eventually stored in toluene (or hexane) in a N_2-filled glovebox. The amount of zinc precursor was varied from 0 mg (Zn/In = 0) to 36 mg (0.18 mmol, Zn/In = 1.5), while keeping the amount of indium and phosphorus precursors constant.

Preparation of In- and Zn-Palmitate and $P(TMS)_3$ Precursors for Core Growth. A stock solution of In- and Zn-palmitate (In:Zn = 1:1) was prepared by mixing 292 mg (1 mmol) of $In(OAc)_3$, 184 mg (1 mmol) of $Zn(OAc)_2$, and 769 mg (3 mmol) of PA in 10 mL of ODE in a three-neck round-bottom flask. The mixture was degassed under vacuum at 130 °C for 2 h and then heated to 250 °C under N_2 in order to form the In- and Zn-palmitate complexes. After complete dissolution of metal precursors, the solution was cooled to room temperature and stored in a N_2-filled glovebox. A $P(TMS)_3$ precursor solution was prepared by diluting 145 μL (0.5 mmol) of $P(TMS)_3$ in 10 mL of ODE.

Growth of Red Emitting InZnP Cores. In order to further increase the size of as-synthesized InZnP QDs, a multiple injection route was adopted. The temperature of the crude "hot" reaction mixture was lowered to 250 °C, and 1 mL of the In-Zn palmitate stock solution was injected dropwise into the flask over 6 min. The solution was held at 250 °C for a further 10 min, after which 1 mL of the $P(TMS)_3$ precursor solution was injected dropwise in the reaction flask over 40 min. The same procedure was followed several times until the particles reached the desired size (see Figure S1a of the Supporting Information, SI).

CE Reaction Involving InZnP QDs and Ga^{3+} Ions. A 0.12 M gallium precursor solution was prepared in a nitrogen-filled glovebox by dissolving $GaCl_3$ (3 mmol, 528 mg) in oleic acid (12 mmol, 3.39 g) and 20 mL ODE at 140 °C for 1 h. The temperature of the crude "hot" reaction mixture was lowered to 200 °C, and 230 μL of gallium precursor solution (containing 0.03 mmol of Ga^{3+}) was added dropwise. The reaction mixture was kept at 200 °C for 1 h, after which another 230 μL of gallium precursor solution was added. Subsequent injections of Ga precursor solution were performed following the same procedure up to a total of 0.15 mmol of $Ga(OA)_3$ added.

Synthesis of InZnP/GaP Core/Shell QDs. After the final addition of Ga precursor in the CE reaction, the temperature of the crude "hot" reaction mixture was reduced to 150 °C and 0.03 mmol of $P(TMS)_3$ diluted in 1 mL of ODE was added. The reaction was then reheated to 200 °C and left to react for 1 h. Subsequent injections of 0.03 mmol of Ga oleate (added at 200 °C) and $P(TMS)_3$ precursors (added at 150 °C) were performed following the same procedure.

Growth of ZnSeS Outer Shell. The selenium and sulfur precursor solutions used for the ZnSeS shell growth were prepared by dissolving 4 mmol of Se or S powder in 4 mL of TOP to give 1 M solutions of TOPSe and TOPS. In a typical shell growth procedure, 0.325 g of Zn stearate and 1.5 mL of ODE were mixed thoroughly in a nitrogen-filled glovebox, loaded into a syringe, and added into a three-neck flask containing 2 mL of as-synthesized InZnP/InGaP/GaP QD solution at room temperature. At this point, the temperature of the crude "hot" reaction mixture was set to 300 °C with a heating rate of 10 °C/min. When the temperature reached 90 °C, a total of 0.5 mL of the anion stock solutions (TOP-Se + TOP-S) were added. The ZnSeS shell composition was changed by varying the TOP-Se and TOP-S precursor ratio. For example, in the case of Se/S = 0, 0.5 mL of 1 M TOP-S was added, while, in case of Se/S = 1, 0.25 mL of 1 M TOP-Se and 0.25 mL of 1 M TOP-S were added. The reaction was kept at 300 °C for 20 min and was subsequently quenched by cooling the flask down to room temperature. The resulting QDs were purified by dispersion in chloroform (2 mL), followed by precipitation by addition of a mixture of ethanol:acetone (1:4). The obtained QDs were stored in toluene in a N_2-filled vial in the glovebox.

Ligand Exchange with S^{2-} ions.[30] The exchange of original organic ligands with S^{2-} inorganic species was carried out in a N_2 glovebox. 20 μL of $(NH_4)_2S$ solution (20% in H_2O) was added to 1 mL of FA and mixed with 1 mL of a purified QD dispersion in toluene. The biphasic mixture was sonicated for 15 min at 60 °C, leading to a complete phase transfer of the NCs from toluene to the FA phase, leaving residual organic ligands and unreacted species in the toluene phase (as they are not soluble in FA). The phase transfer can be easily monitored by the color change. The FA phase, which now contains only the inorganic QDs, was separated and acetone was added as nonsolvent to precipitate the ligand exchanged QDs. To remove eventual residual organic ligands, the QDs were further washed twice with toluene. Eventually, the QDs were precipitated a last time by adding acetone and redispersed in DMF and stored in a N_2-filled vial in the glovebox for further analysis.

UV−vis Absorption and PL Emission Measurements. QD samples for optical analysis were prepared by diluting the purified stock solutions in toluene in a 1 cm quartz cuvette. UV−vis absorption spectra were measured with a PerkinElmer Lambda 40 UV/vis spectrometer. PL emission spectra were obtained using a PTI QuantaMaster with a 75 W xenon lamp, using an excitation wavelength of 450 nm.

Absolute PL QY Measurements. QD samples for PL QY measurements were prepared by diluting the purified stock solutions in toluene. The PL QY of the QDs was determined using an integrated sphere setup at Philips Research Laboratory. The setup consisted of a 445 nm diode laser, a Labsphere 6″ integrating sphere, and a fiber coupled spectrometer (USB 4000, Ocean Optics). The combination of sphere, fiber, and spectrometer was calibrated with a light source of known emission characteristics.

Transmission Electron Microscopy (TEM). TEM micrographs were acquired using a JEOL microscope operating at 120 kV (bright-field images) or a FEI Technai G2 F20 microscope at 200 kV (dark-field images). Samples for TEM imaging were prepared by drop-casting a toluene solution of QDs onto a carbon-coated copper (400-mesh) TEM grid. The TEM micrographs were used to estimate the

DOI: 10.1021/acs.chemmater.7b00848
Chem. Mater. 2017, 29, 5192−5199

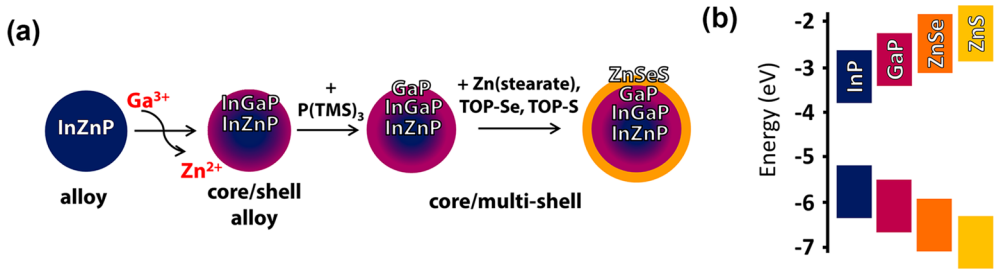

Figure 1. (a) Sketch of the different steps for the synthesis of InZnP/InGaP/ZnSeS core/shell QDs. Subscripts denoting cation and anion stoichiometry have been omitted for clarity. (b) Schematic of a Type-I band alignment in the case of our core/shell QDs.

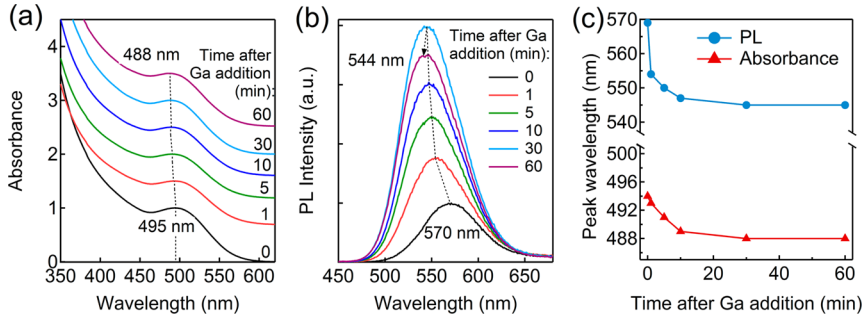

Figure 2. Change in InZnP QD (Zn/In = 1) absorbance and PL over 1 h at 200 °C after addition of 0.03 mmol of $Ga(OA)_3$. (a) Absorbance of aliquots removed at specific times noted on graph. Time = 0 min is before addition of $Ga(OA)_3$. Traces are offset with increasing time, and dotted line indicates the trend in peak wavelength. (b) PL intensity as a function of time, normalized to the fraction of light absorbed at the excitation wavelength of 400 nm. (c) Peak absorbance and PL wavelengths plotted as a function of time after Ga addition.

size of the QDs and the numbers of shell monolayers (MLs) grown of GaP or ZnSeS. This was done by considering half of the zinc blende GaP and ZnSeS lattice parameters. For GaP, this value is 0.542 nm,[31] and for ZnSeS, it varies with the Se/S ratio (see SI, Figure S6; for example, Se/S = 4 gives 0.557 nm).[13,32]

Inductively Coupled Plasma (ICP) Optical Emission Spectroscopy (OES) Elemental Analysis. ICP measurements to obtain Zn/In and Ga/In ratios were carried out using an iCAP 6500 Thermo spectrometer. All chemical analyses performed by ICP-OES were affected by a systematic error of about 5%. Samples were dissolved in HCl/HNO_3 3:1 (v/v).

RESULTS AND DISCUSSION

The Reaction of Gallium Oleate with InZnP QDs. InZnP alloy QDs were prepared following the procedure described in our previous work (see the Experimental Methods section for details).[26] Red emitting InZnP QDs were synthesized by performing multiple injections of P and Zn-In precursors on as-synthesized cores (see the Experimental Methods section for details). ICP and XRD measurements confirmed that the resulting NCs retained the same composition (Zn/In ratio) and the same lattice constants as the starting InZnP seeds (see Figure S1b,c of the SI).[26]

To investigate the effects of the cation exchange (CE) reaction between InZnP QDs and gallium ions,[27] gallium oleate ($Ga(OA)_3$) was added in 0.03 mmol increments to as-synthesized samples of InZnP QDs with varying Zn/In feed ratios at 200 °C, and the optical properties of the resulting QDs were monitored. We note that $P(TMS)_3$ (0.06 mmol) is the limiting reagent in the InZnP QD synthesis, so there should be a similar total number of Zn + In cations incorporated into the QDs for all samples irrespective of the Zn/In feed ratios. Figure 2a–c presents the absorbance and PL of InZnP QDs (Zn/In = 1) as a function of time after the addition of 0.03 mmol of $Ga(OA)_3$. The absorbance and PL peaks are initially at 495 and 570 nm, respectively, and both undergo a blue-shift over 30–60 min to new values of 487 and 544 nm, respectively. At the same time, the PL intensity also increases markedly.

Increasing quantities of $Ga(OA)_3$ were then added to InZnP QDs with varying Zn/In feed ratios of 0, 0.5, and 1.5. The $Ga(OA)_3$ was added in 0.03 mmol increments per hour up to a total of 0.15 mmol; significantly faster addition rates led to degradation of the QDs. The normalized UV–vis absorption spectra acquired during these experiments are reported in Figure 3a–c. The absorption spectra of as-synthesized InZnP NCs (black spectra) are characterized by 1S exciton absorption peaks which remain clearly defined upon addition of $Ga(OA)_3$.[33]

The addition of $Ga(OA)_3$ to pure InP (Zn/In = 0) QDs causes a systematic red-shift and a broadening of their absorption onset (see Figure 3a). On the other hand, in the case of zinc containing InZnP QDs, a systematic blue-shift of the exciton peak is observed upon addition of $Ga(OA)_3$ up to 0.12 mmol, followed by a red-shift upon further addition of gallium precursor (see Figure 3b,c). The magnitude of the blue-shift of the exciton peak is more pronounced in samples with higher Zn content (10 and 30 nm for Zn/In = 0.5 and Zn/In = 1.5, respectively). Heating InZnP QDs for the same time in the absence of $Ga(OA)_3$ does not lead to a blue-shift of the absorbance (see the Supporting Information, Figure S3a).

The occurrence of a blue-shift upon adding $Ga(OA)_3$ as a source of gallium ions to InZnP QDs has been previously discussed by Kim et al.,[27] who attributed it to a CE reaction between In^{3+} and Ga^{3+} ions in the outer layers of the QDs that resulted in a decrease of the InP core size, and thus, in a more pronounced quantum confinement.[27,34] However, the same explanation cannot be applied here, as we would have observed a similar blue-shift for both InP and InZnP QDs upon exposure to $Ga(OA)_3$, which is not the case (see Figure 3a). Our results,

DOI: 10.1021/acs.chemmater.7b00848
Chem. Mater. 2017, 29, 5192–5199

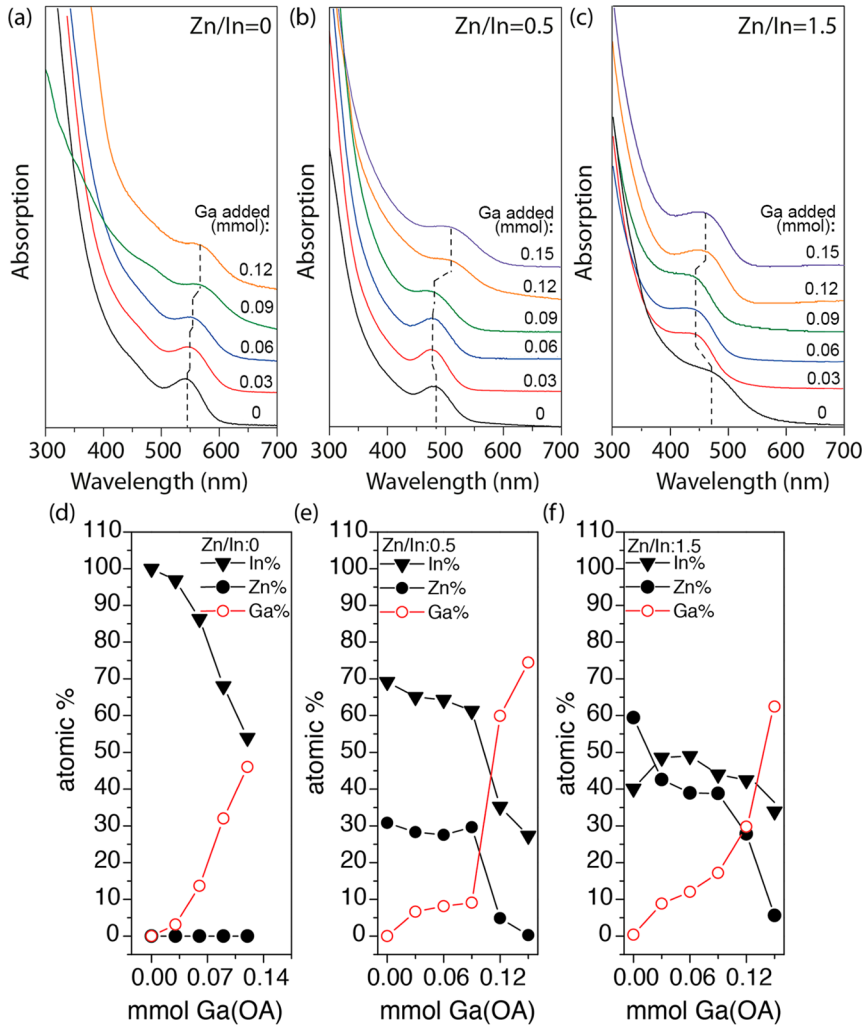

Figure 3. (a–c) Absorption spectra of InZnP QDs with varying initial concentrations of Zn at different stages during the addition of $Ga(OA)_3$. (d–f) The relative In, Zn, and Ga content measured using ICP in the InZnP + $Ga(OA)_3$ QDs as a function of the amount of $Ga(OA)_3$ added, for purified cores with different Zn/In feed ratios: (d) 0, (e) 0.5, and (f) 1.5.

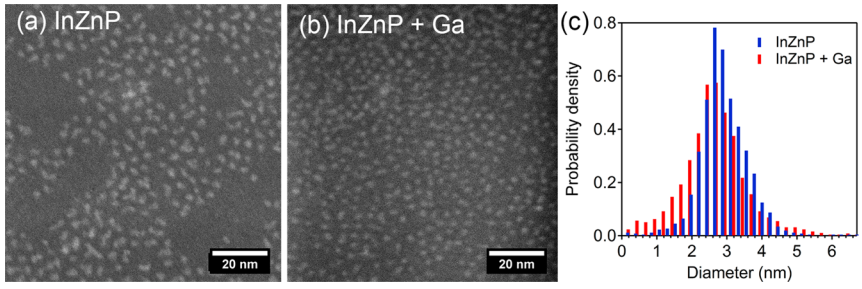

Figure 4. Dark-field scanning transmission electron microscopy images of (a) InZnP QDs with a Zn/In ratio of 1.5 and (b) the same QDs after addition of 0.09 mmol of $Ga(OA)_3$ at 200 °C over 3 h. (c) Size distribution of measured QD diameters (>1000 measurements per sample) from the InZnP sample (blue) and the InZnP + Ga sample (red).

therefore, suggest that the amount of Zn inside the starting QDs plays an important role in the reaction with Ga^{3+} ions.

To explain the evolution of the optical features of the QDs upon reaction with $Ga(OA)_3$, we measured their composition with ICP elemental analysis, before and after the addition of gallium precursor, with particular attention to Zn/In and Ga/In ratios. The data for each $Ga(OA)_3$ amount was acquired from separate reactions starting from the same cores. To ensure the complete removal of unreacted species before the elemental analysis, the QDs were carefully washed and the organic ligands were replaced with S^{2-} ions through the addition of $(NH_4)_2S$ (see Experimental Methods for details).[30] The results of ICP analysis are summarized in Figure 3d–f. As described in our previous report,[26] the measured initial Zn/In ratio in the QDs closely matches the feed ratio. In all of the InZnP QD samples, the relative amount of Ga in the QDs increases with the amount of gallium precursor added. For samples containing zinc, the relative zinc content decreases upon addition of

DOI: 10.1021/acs.chemmater.7b00848
Chem. Mater. 2017, 29, 5192–5199

$Ga(OA)_3$ (see Figure 3e,f), dropping almost to zero after the addition of large amounts of $Ga(OA)_3$ (0.15 mmol). The relative indium content is also reduced with the addition of $Ga(OA)_3$, but much less so than the Zn content. Furthermore, the magnitude of the change depends on the starting Zn/In ratio. In QDs with low Zn/In ratios (Zn/In = 0, 0.5), a significant reduction in relative indium content is observed (see Figure 3d,e), whereas the relative indium content only drops slightly with Zn/In = 1.5 (see Figure 3f). The trends in the ICP data were reproducible (see the Supporting Information, Figure S4, for data from additional experiments).

Taken together, the ICP and absorbance results suggest that a preferential $Ga^{3+} \rightarrow Zn^{2+}$ CE reaction occurs. The replacement of zinc with gallium observed for samples with Zn/In $\geq$ 0.5 suggests the formation of graded-composition InZnP/InGaP nanocrystals via CE which would have an increasing band gap toward the QD surface, consistent with the observed absorbance blue-shift (see Figure 3b,c). Such core−shell structures are often observed in systems with low ion diffusivity where the reaction starts from the QD surface.[35−37] Indeed, the 30−60 min time required for the CE reaction to reach completion (Figure 2c) suggests slow ion diffusion, an observation supported by other reports of slow CE reactions in III−V QD materials.[37,38]

TEM images of InZnP QDs (Zn/In = 1.5) taken before and after addition of 0.09 mmol of $Ga(OA)_3$, at which point the absorbance blue-shift was maximized, are shown in Figure 4a,b, respectively. Histograms of measured QD diameters for each sample (see Figure 4c, >1000 measurements per sample) show that the QD size distribution did not change significantly during the CE reaction after 0.09 mmol of $Ga(OA)_3$ was added: the initial average particle diameter (± one standard deviation) for InZnP was 2.8 nm ± 0.5 nm, and after $Ga(OA)_3$ addition, it was 2.6 nm ± 0.6 nm. However, further addition of $Ga(OA)_3$ up to 0.15 mmol results in a broadening and red-shift of the exciton peak (see Figure 3b,c), suggesting that the QDs undergo growth via Ostwald ripening later in the CE reaction, whereby the largest QDs grow via consumption of smaller ones.[13,39]

The preferential $Ga^{3+} \rightarrow Zn^{2+}$ CE can be rationalized as follows: (i) Zn^{2+} is a weaker Lewis acid than In^{3+} and Ga^{3+} (their respective chemical hardnesses η are 10.9, 13, and 17 eV).[40] Therefore, according to Pearson's hard soft acid base (HSAB) theory,[41] zinc ions have a stronger affinity to the oleic acid (weak Lewis base, η = 6.4 eV)[40] present in the reaction mixture, and so they can be selectively extracted and replaced by Ga^{3+} ions.[35,36,38,42−46] Indeed, it has been previously reported that carboxylic acids can favor the selective replacement of Zn^{2+} ions with stronger Lewis acids in QDs.[47,48] (ii) The cation exchange reaction could also be dictated by thermodynamic factors: although no lattice energy values were found for InZnP and InGaP compounds, InZnP is a metastable phase and we can speculate that its lattice energy is most likely lower than that of InGaP, which is a very stable alloy.[17,26]

We remark that the substitution of Zn^{2+} with Ga^{3+} cations should lead to an excess of positive charges in the resulting QDs. In an earlier publication,[26] we have discussed the possibilities for maintaining charge neutrality in InP QDs when replacing In^{3+} with Zn^{2+}, such as the formation of phosphorus vacancies[49] or a combination of interstitial and substitutional zinc,[50] and these processes could feasibly be reversed during the Ga^{3+} CE reaction. However, as InZnP/InGaP QDs are passivated by negatively charged X-type oleate surfactants, a change in the surface ligand density can also possibly restore charge neutrality.[51,52]

Although an increase in the overall Ga/In ratio was observed for the Zn/In = 0 sample upon addition of $Ga(OA)_3$, the concurrent red-shift of the QD absorbance rules out the formation of a higher-band-gap InGaP material via $Ga^{3+} \rightarrow In^{3+}$ CE (see Figure 3d). The broadening and red-shift of the absorbance band suggests that growth by Ostwald ripening may also occur for InP QDs upon reaction with the gallium precursor. Indeed, analysis of TEM images confirms that the InP QD diameter increases after the addition of 0.12 mmol of $Ga(OA)_3$ (see Figure S2 of the SI). In addition, the large excess of $Ga(OA)_3$ should lead to the full passivation of surface anion sites with gallium oleate, which could induce a red-shift in the InP QDs similar to that recently observed by Stein et al.[53] for cadmium oleate capped InP QDs. Both of these processes would explain the increase the relative gallium content, and subsequent decrease in relative indium content, observed for InP in Figure 3d. We note that these processes can also account for the decrease in relative indium content observed for the Zn/In $\geq$ 0.5 samples (see Figure 3e,f).

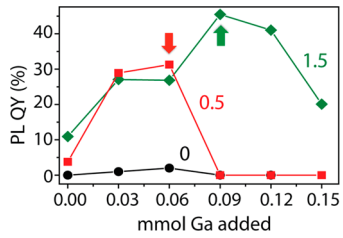

Figure 5. Plot of the PL QY of InZnP/InGaP QDs with different initial Zn/In ratios (0, black dots; 0.5, red squares; 1.5, green diamonds) as a function of the amount of Ga precursor added. The arrows highlight the point of maximum PL QY for each sample.

Effect of the CE with Ga^{3+} Ions on the Photoluminescence. In Figure 5, we show the change in PL QY of InZnP QDs with varying Zn/In ratios during the addition of $Ga(OA)_3$. While no enhancement of the PL QY was observed for InP QDs (see Figure 5, black curve), the PL of InZnP increased after the CE with Ga^{3+} ions (see Figure 5, red and green curves). In the case of InZnP with a Zn/In ratio of 1.5, the PL QY of the QDs increased from ∼5% up to 40% after the addition of 0.09 mmol of $Ga(OA)_3$, while a further increase in the amount of $Ga(OA)_3$ resulted in a decrease of the PL QY. Heating InZnP QDs without addition of $Ga(OA)_3$ resulted in the PL QY slowly increasing to 1.7 times its initial value after 3.5 h, then decreasing at longer times (see Figure S3 of the SI), which is not enough to account for the PL increases observed in Figure 5. For samples with Zn/In between zero and 0.5, no PL increase was observed upon Ga^{3+} addition (see Figure S3 of the SI).

The increase in PL QY accompanying the reaction of InZnP with $Ga(OA)_3$ further supports the hypothesis that the $Ga^{3+} \rightarrow Zn^{2+}$ CE starts from the surface to form graded-composition core/shell heterostructures with high PL QY due to reduced interfacial strain.[8,54] As the CE between Zn^{2+} and Ga^{3+} ions approached completion, i.e., after the addition of a more than 0.12 mmol Ga precursor (see Figure 3e,f), the PL QY began to decrease (see Figure 5). The observed decrease in PL QY was concurrent with the absorbance red-shift and broadening

DOI: 10.1021/acs.chemmater.7b00848
Chem. Mater. 2017, 29, 5192−5199

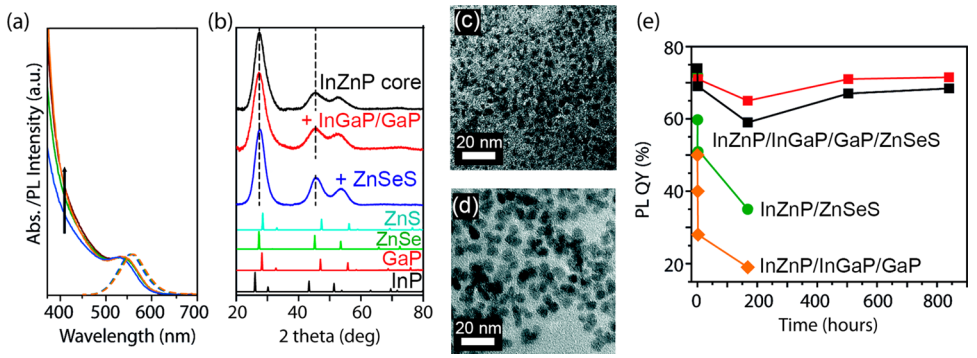

Figure 6. (a) Absorption (solid line) and emission (dashed line) spectra of InZnP/InGaP/GaP/ZnSeS core/shell QDs at different stages during the growth of a ZnSeS shell. (b) XRD patterns obtained from drop-cast solutions of InZnP (Zn/In = 1.5) QDs (black), InZnP/InGaP/GaP QDs (red), and InZnP/GaP/ZnSeS QDs (blue). The corresponding bulk reflections of zinc blende InP (black, ICSD code 24517), GaP (red, ICSD code 77087), ZnSe (green, ICSD code 77091), and ZnS (light blue, ICSD code 67453) are reported in the lower panels. (c, d) TEM images of InZnP/InGaP/GaP/ZnSeS QDs. (e) Plots of the PL QY for four suspensions of QDs kept under constant UV irradiation (UV lamp (1 W/cm^2)), as a function of the irradiation time. Four samples were measured: two batches of purified InZnP/InGaP/GaP/ZnSeS QDs (red and black squares), InZnP/ZnSeS QDs (green dots), and InZnP/InGaP/GaP QDs (orange diamonds).

attributed to Ostwald ripening (see Figure 3b,c), indicating that this process generates defects or lattice strain, which impedes further improvement of the PL QY.[54]

With the aim of further enhancing the PL QY of our QDs, a GaP shell was deliberately grown on cation exchanged InZnP/InGaP QDs by injecting subsequent amounts of phosphorus ($P(TMS)_3$) and gallium ($Ga(OA)_3$) precursors into the crude reaction mixture (see the Experimental Methods for details). The deliberate shell growth was performed on samples where an optimal amount of $Ga(OA)_3$ had been added during the CE, i.e., when the PL QY is highest and prior to the onset of the absorbance red-shift. We observed that the PL QY of the QDs increased to a maximum value of 55%, for cores with Zn/In = 1.5 subjected to the CE reaction with 0.09 mmol of $Ga(OA)_3$ and addition of 0.03 mmol of $P(TMS)_3$ precursor. Further growth of the GaP shell by subsequent Ga and P precursor additions resulted in a broader and a less efficient PL emission (see Figure S5a,b of the SI for optical characterization of the InZnP/InGaP/GaP QDs). This behavior can be rationalized considering that, as the GaP shell becomes thicker, the lattice mismatch between the core and the shell can induce interfacial lattice strain, which could lead to the formation of defects and a reduction of the PL QY.[55,56]

Synthesis of InZnP/InGaP/GaP/ZnSeS Core/Multishell QDs. Finally, an outer layer of a robust wide-band-gap material was grown onto the InZnP/InGaP/GaP QDs to improve their photostability and PL QY (see schematic in Figure 1a,b). To minimize the lattice mismatch between the core and the shell materials, we chose ZnSeS as a wide-band-gap shell material, for which the lattice constant can be tuned by adjusting the ratio of Se/S.[26,32] After determining the lattice constant of InZnP/InGaP/GaP QDs using XRD, we calculated the optimum ratio of Se and S precursors to grow a lattice matched ZnSeS shell.[26] The shell was grown by injecting zinc stearate, TOPSe and TOPS precursors directly into the InZnP/InGaP/GaP QDs crude reaction mixture (see Figure S6 of the SI and the Experimental Methods section for details).

Figure 6a shows the absorption and PL emission spectra of InZnP/InGaP/GaP/ZnSeS core/multishell QDs at different reaction times during shell growth. As first proof of the shell growth, a marked increase of the absorbance at wavelengths below 440 nm was observed, corresponding to the band gap of bulk ZnSeS.[32] Figure 6b shows the XRD patterns acquired for InZnP QDs (black pattern), InZnP/InGaP/GaP QDs (red pattern), and InZnP/InGaP/GaP/ZnSeS QDs (blue pattern), which confirms that the three samples have a zinc blende crystal structure with the same lattice constant, as no shift of XRD peaks was observed. This suggests the lattice constant of the InZnP QDs does not change during Ga CE reaction. The Ga^{3+} cation is similar in size to Zn^{2+}, and both are smaller than In^{3+},[26,57] so the CE reaction appears to preserve the InZnP similar lattice constant within the resolution of our measurements. TEM analysis further supports the formation of a ZnSeS shell as the mean diameter of the QDs increased from 3.5 nm up to 4.6 ± 0.6 nm (see Figure 6c, and Figure S7a of the SI).

The resulting QDs were characterized by a PL emission peak at 565 nm with a full width at half-maximum (fwhm) of 52 nm, and a PL QY of up to 75% (see Figure 6a). These values are slightly inferior to those reported by Kim et al. for a similar core/multishell system,[27,28] but we note that we have focused on understanding the Ga^{3+} cation exchange reaction and have not optimized our synthesis parameters for maximum PL QY. Core/shell QDs emitting at longer wavelengths (up to 620 nm) were also synthesized by using red emitting InZnP cores (see the Experimental Methods sections for details and Figure S7b of the SI).

The stability of these multishell samples was tested with a setup at Philips Research Laboratories. Dispersions of purified InZnP/InGaP/GaP QDs, InZnP/ZnSeS QDs, and InZnP/InGaP/GaP/ZnSeS QDs in toluene were loaded, under ambient conditions, into different capillaries, placed on the top of a GaN LED (lamp power 1 W/cm^2; temperature 50−60 °C), and the PL QY of the samples was monitored for 5 weeks. These conditions mimic those of remote phosphors used in LED lamps. The results are summarized in Figure 6e. In the case of InZnP/InGaP/GaP and InZnP/ZnSeS QDs, the PL QY drastically decreases after only 1 h of exposure. On the other hand, InZnP/InGaP/GaP/ZnSeS QDs showed prolonged stability as the PL QY, after an initial small drop of about 5% in the first hour, retained a constant PL QY of 70% for 5 weeks. This demonstrates that multishell InZnP/InGaP/GaP/ZnSeS QDs have a superior photostability due to the Type I configuration afforded by the GaP and ZnSeS shells. From these results, it is evident that this system can be a highly promising candidate as a Cd-free phosphor.

DOI: 10.1021/acs.chemmater.7b00848
Chem. Mater. 2017, 29, 5192−5199

CONCLUSIONS

In summary, we have shown that the addition of Ga^{3+} ions to pristine InZnP QDs can increase the PL QY of such systems from ~5% up to 55%, but that a Zn/In ratio of at least 0.5 in the starting InZnP QDs is pivotal to achieving high PL QYs. This is the result of a preferential cation exchange reaction between Zn^{2+} and Ga^{3+} ions, which leads to the formation of a higher-band-gap InGaP surface layer that enhances the PL QY and blue-shifts the absorbance of the resulting QDs. We have also argued that CE between In^{3+} and Ga^{3+} does not occur, evidenced by the broadening and red-shifting of absorbance and lack of PL increase when samples with Zn/In ratios lower than 0.5 are exposed to Ga^{3+} ions. Further increases in the PL QY (up to 75%) and prolonged photostability were afforded by growth of a GaP shell and a ZnSeS shell with a composition chosen to match the lattice of the InZnP/InGaP/GaP QD. From a practical point of view, these results demonstrate that cation exchange reactions in InZnP-based QDs can narrow the gap between the performance of Cd-free LED phosphors and industrial requirements for LED phosphors.

ASSOCIATED CONTENT

Supporting Information

The Supporting Information is available free of charge on the ACS Publications website at DOI: 10.1021/acs.chemmater.7b00848.

Extended optical characterization of samples, TEM images for Zn/In = 0 samples, and ICP data for additional reactions (PDF)

AUTHOR INFORMATION

Corresponding Author

*E-mail: A.J.Houtepen@tudelft.nl.

ORCID

Nicholas Kirkwood: 0000-0002-7845-7081

Luca De Trizio: 0000-0002-1514-6358

Liberato Manna: 0000-0003-4386-7985

Author Contributions

The manuscript was written through contributions of all authors. All authors have given approval to the final version of the manuscript.

Author Contributions

#These authors contributed equally.

Notes

The authors declare no competing financial interest.

ACKNOWLEDGMENTS

This research is supported by the Dutch Technology Foundation STW, which is part of The Netherlands Organization for Scientific Research (NWO), and which is partly funded by Ministry of Economic Affairs, and by the seventh European Community Framework Program under grant agreement no. 614897 (ERC Consolidator Grant "TRANS-NANO"). The research leading to these results has received funding from the European Research Council Horizon 2020 ERC Grant Agreement No. 678004.

REFERENCES

(1) Mashford, B. S.; Stevenson, M.; Popovic, Z.; Hamilton, C.; Zhou, Z.; Breen, C.; Steckel, J.; Bulovic, V.; Bawendi, M.; Coe-Sullivan, S.; et al. High-efficiency quantum-dot light-emitting devices with enhanced charge injection. *Nat. Photonics* **2013**, *7*, 407−412.

(2) Lee, K.-H. H.; Lee, J.-H. H.; Kang, H.-D. D.; Park, B.; Kwon, Y.; Ko, H.; Lee, C.; Lee, J.; Yang, H. Over 40 cd/A efficient green quantum dot electroluminescent device comprising uniquely large-sized quantum dots. *ACS Nano* **2014**, *8*, 4893−4901.

(3) Gur, I.; Fromer, N. A.; Geier, M. L.; Alivisatos, A. P. Air-stable all-inorganic nanocrystal solar cells processed from solution. *Science* **2005**, *310*, 462−465.

(4) de Mello Donegá, C. Synthesis and properties of colloidal heteronanocrystals. *Chem. Soc. Rev.* **2011**, *40*, 1512−1546.

(5) Chen, O.; Zhao, J.; Chauhan, V. P.; Cui, J.; Wong, C.; Harris, D. K.; Wei, H.; Han, H.-S. S.; Fukumura, D.; Jain, R. K.; et al. Compact high-quality CdSe-CdS core-shell nanocrystals with narrow emission linewidths and suppressed blinking. *Nat. Mater.* **2013**, *12*, 445−451.

(6) Cirillo, M.; Aubert, T.; Gomes, R.; Van Deun, R.; Emplit, P.; Biermann, A.; Lange, H.; Thomsen, C.; Brainis, E.; Hens, Z. Flash" Synthesis of CdSe/CdS Core−Shell Quantum Dots. *Chem. Mater.* **2014**, *26*, 1154−1160.

(7) Carbone, L.; Cozzoli, P. Colloidal heterostructured nanocrystals: synthesis and growth mechanisms. *Nano Today* **2010**, *5*, 449−493.

(8) Boldt, K.; Kirkwood, N.; Beane, G. A.; Mulvaney, P. Synthesis of Highly Luminescent and Photo-Stable, Graded Shell CdSe/CdxZn1−xS Nanoparticles by In Situ Alloying. *Chem. Mater.* **2013**, *25*, 4731−4738.

(9) Alivisatos, A. Semiconductor clusters, nanocrystals, and quantum dots. *Science* **1996**, *271*, 933−938.

(10) Yang, X.; Zhao, D.; Leck, K.; Tan, S.; Tang, Y.; Zhao, J.; Demir, H.; Sun, X. Full Visible Range Covering InP/ZnS Nanocrystals with High Photometric Performance and Their Application to White Quantum Dot Light-Emitting Diodes. *Adv. Mater.* **2012**, *24*, 4180−4185.

(11) Xu, S.; Ziegler, J.; Nann, T. Rapid synthesis of highly luminescent InP and InP/ZnS nanocrystals. *J. Mater. Chem.* **2008**, *18*, 2653−2656.

(12) Thuy, U.; Reiss, P.; Liem, N. Luminescence properties of In(Zn)P alloy core/ZnS shell quantum dots. *Appl. Phys. Lett.* **2010**, *97*, 193104.

(13) Tamang, S.; Lincheneau, C.; Hermans, Y.; Jeong, S.; Reiss, P. Chemistry of InP Nanocrystal Syntheses. *Chem. Mater.* **2016**, *28*, 2491−2506.

(14) Song, W.-S.; Lee, H.-S.; Lee, J. C.; Jang, D. S.; Choi, Y.; Choi, M.; Yang, H. Amine-derived synthetic approach to color-tunable InP/ZnS quantum dots with high fluorescent qualities. *J. Nanopart. Res.* **2013**, *15*, 1750.

(15) Soenen, S.; Manshian, B.; Aubert, T.; Himmelreich, U.; Demeester, J.; De Smedt, S. C.; Hens, Z.; Braeckmans, K. Cytotoxicity of cadmium-free quantum dots and their use in cell bioimaging. *Chem. Res. Toxicol.* **2014**, *27*, 1050−1059.

(16) Mutlugun, E.; Hernandez-Martinez, P.; Eroglu, C.; Coskun, Y.; Erdem, T.; Sharma, V. K.; Unal, E.; Panda, S. K.; Hickey, S. G.; Gaponik, N.; Eychmuller, A.; Demir, H. V. Large-area (over 50 cm x 50 cm) freestanding films of colloidal InP/ZnS quantum dots. *Nano Lett.* **2012**, *12*, 3986−3993.

(17) Mushonga, P.; Onani, M.; Madiehe, A.; Meyer, M. Indium phosphide-based semiconductor nanocrystals and their applications. *J. Nanomater.* **2012**, *2012*, 869284.

(18) Lim, J.; Bae, W.; Lee, D.; Nam, M.; Jung, J.; Lee, C.; Char, K.; Lee, S. InP@ ZnSeS, core@ composition gradient shell quantum dots with enhanced stability. *Chem. Mater.* **2011**, *23*, 4459−4463.

(19) Lim, J.; Park, M.; Bae, W.; Lee, D.; Lee, S.; Lee, C.; Char, K. Highly Efficient Cadmium-Free Quantum Dot Light-Emitting Diodes Enabled by the Direct Formation of Excitons within InP@ZnSeS Quantum Dots. *ACS Nano* **2013**, *7*, 9019−9026.

(20) Li, L.; Reiss, P. One-pot synthesis of highly luminescent InP/ZnS nanocrystals without precursor injection. *J. Am. Chem. Soc.* **2008**, *130*, 11588−11589.

(21) Kim, T.; Kim, S.; Kang, M.; Kim, S. Large-scale synthesis of InPZnS alloy quantum dots with dodecanethiol as a composition controller. *J. Phys. Chem. Lett.* **2012**, *3*, 214−218.
(22) Kim, K.; Lee, H.; Ahn, J.; Jeong, S. Highly luminescing multi-shell semiconductor nanocrystals InP/ZnSe/ZnS. *Appl. Phys. Lett.* **2012**, *101*, 073107.
(23) Dennis, A. M.; Mangum, B. D.; Piryatinski, A.; Park, Y.-S.; Hannah, D. C.; Casson, J. L.; Williams, D. J.; Schaller, R. D.; Htoon, H.; Hollingsworth, J. A. Suppressed Blinking and Auger Recombination in Near-Infrared Type-II InP/CdS Nanocrystal Quantum Dots. *Nano Lett.* **2012**, *12*, 5545−5551.
(24) *Indium Phosphide and Related Materials: Processing, Technology, and Devices*; Katz, A., Ed.; Artech House Inc.: Boston, MA, 1992.
(25) Anc, M. J.; Pickett, N. L.; Gresty, N. C.; Harris, J. A.; Mishra, K C. Progress in non-Cd quantum dot development for lighting applications. *ECS J. Solid State Sci. Technol.* **2013**, *2*, R3071−R3082.
(26) Pietra, F.; De Trizio, L.; Hoekstra, A. W.; Renaud, N.; Prato, M.; Grozema, F. C.; Baesjou, P. J.; Koole, R.; Manna, L.; Houtepen, A. J. Tuning the Lattice Parameter of InxZnyP for Highly Luminescent Lattice-Matched Core/Shell Quantum Dots. *ACS Nano* **2016**, *10*, 4754−4762.
(27) Kim, S.; Kim, T.; Kang, M.; Kwak, S.; Yoo, T.; Park, L.; Yang, I.; Hwang, S.; Lee, J.; Kim, S.; et al. Highly Luminescent InP/GaP/ZnS Nanocrystals and Their Application to White Light-Emitting Diodes. *J. Am. Chem. Soc.* **2012**, *134*, 3804−3809.
(28) Park, J. P.; Lee, J.-J.; Kim, S.-W. Highly luminescent InP/GaP/ZnS QDs emitting in the entire color range via a heating up process. *Sci. Rep.* **2016**, *6*, 30094.
(29) Bae, W.; Padilha, L. A.; Park, Y.-S.; McDaniel, H.; Robel, I.; Pietryga, J. M.; Klimov, V. I. Controlled Alloying of the Core−Shell Interface in CdSe/CdS Quantum Dots for Suppression of Auger Recombination. *ACS Nano* **2013**, *7*, 3411−3419.
(30) Nag, A.; Kovalenko, M. V.; Lee, J.-S. S.; Liu, W.; Spokoyny, B.; Talapin, D. V. Metal-free inorganic ligands for colloidal nanocrystals: S2-, HS-, Se2-, HSe-, Te2-, HTe-, TeS3(2-), OH-, and NH2- as surface ligands. *J. Am. Chem. Soc.* **2011**, *133*, 10612−10620.
(31) Rabadanov, M.; Loshmanov, A.; Shaldin, Yu. V. Anharmonic thermal vibrations of atoms in crystals with sphalerite structure-GaP, ZnS, ZnSe, and ZnTe: High-temperature x-ray structure studies. *Crystallogr. Rep.* **1997**, *42*, 592−602.
(32) Sadekar, H.; Ghule, A.; Sharma, R. Bandgap engineering by substitution of S by Se in nanostructured ZnS 1− x Se x thin films grown by soft chemical route for nontoxic optoelectronic device applications. *J. Alloys Compd.* **2011**, *509*, 5525−5531.
(33) Fu, H.; Zunger, A. InP quantum dots: Electronic structure, surface effects, and the redshifted emission. *Phys. Rev. B: Condens. Matter Mater. Phys.* **1997**, *56*, 1496.
(34) Baskoutas, S.; Terzis, A. F. Size-dependent band gap of colloidal quantum dots. *J. Appl. Phys.* **2006**, *99*, 013708.
(35) Zhang, J.; Chernomordik, B. D.; Crisp, R. W.; Kroupa, D. M.; Luther, J. M.; Miller, E. M.; Gao, J.; Beard, M. C. Preparation of Cd/Pb Chalcogenide Heterostructured Janus Particles via Controllable Cation Exchange. *ACS Nano* **2015**, *9*, 7151−7163.
(36) De Trizio, L.; Manna, L. Forging Colloidal Nanostructures via Cation Exchange Reactions. *Chem. Rev.* **2016**, *116*, 10852−10887.
(37) De Trizio, D. L.; Gaspari, R.; Bertoni, G.; Kriegel, I.; Moretti, L.; Scotognella, F.; Maserati, L.; Zhang, Y.; Messina, G. C.; Prato, M.; Marras, S.; Cavalli, A.; Manna, L. Cu3-xP Nanocrystals as a Material Platform for Near-Infrared Plasmonics and Cation Exchange Reactions. *Chem. Mater.* **2015**, *27*, 1120−1128.
(38) Beberwyck, B. J.; Alivisatos, P. A. Ion Exchange Synthesis of III−V Nanocrystals. *J. Am. Chem. Soc.* **2012**, *134*, 19977−19980.
(39) Kahlweit, M. Ostwald ripening of precipitates. *Adv. Colloid Interface Sci.* **1975**, *5*, 1−35.
(40) Pearson, R. G. Absolute electronegativity and hardness: application to inorganic chemistry. *Inorg. Chem.* **1988**, *27*, 734−740.
(41) Pearson, R. G. Hard and soft acids and bases. *J. Am. Chem. Soc.* **1963**, *85* (22), 3533−3539.
(42) Luther, J. M.; Zheng, H.; Sadtler, B.; Alivisatos, P. A. Synthesis of PbS Nanorods and Other Ionic Nanocrystals of Complex Morphology by Sequential Cation Exchange Reactions. *J. Am. Chem. Soc.* **2009**, *131*, 16851−16857.
(43) Kovalenko, M.; Schaller, R.; Jarzab, D.; Loi, M. A.; Talapin, D. V. Inorganically functionalized PbS−CdS colloidal nanocrystals: integration into amorphous chalcogenide glass and luminescent properties. *J. Am. Chem. Soc.* **2012**, *134*, 2457−2460.
(44) Justo, Y.; Goris, B.; Kamal, J. S.; Geiregat, P.; Bals, S.; Hens, Z. Multiple dot-in-rod PbS/CdS heterostructures with high photoluminescence quantum yield in the near-infrared. *J. Am. Chem. Soc.* **2012**, *134*, 5484−5487.
(45) Justo, Y.; Sagar, L.; Flamee, S.; Zhao, Q.; Vantomme, A.; Hens, Z. Less Is More. Cation Exchange and the Chemistry of the Nanocrystal Surface. *ACS Nano* **2014**, *8*, 7948−7957.
(46) Casavola, M.; van Huis, M. A.; Bals, S.; Lambert, K.; Hens, Z.; Vanmaekelbergh, D. Anisotropic cation exchange in PbSe/CdSe core/shell nanocrystals of different geometry. *Chem. Mater.* **2012**, *24*, 294−302.
(47) Rivest, J.; Jain, P. Cation exchange on the nanoscale: an emerging technique for new material synthesis, device fabrication, and chemical sensing. *Chem. Soc. Rev.* **2013**, *42*, 89−96.
(48) Groeneveld, E.; Witteman, L.; Lefferts, M.; Ke, X.; Bals, S.; Van Tendeloo, G.; de Mello Donega, C. Tailoring ZnSe-CdSe colloidal quantum dots via cation exchange: from core/shell to alloy nanocrystals. *ACS Nano* **2013**, *7*, 7913−7930.
(49) Chan, L.; Yu, K. M.; Ben-Tzur, M.; Haller, E.; Jaklevic, J.; Walukiewicz, W.; Hanson, C. Lattice location of diffused Zn atoms in GaAs and InP single crystals. *J. Appl. Phys.* **1991**, *69*, 2998−3006.
(50) Krause, H.; Lux, M.; Nowak, E.; Vogt, J.; Flagmeyer, R.; Kühn, G.; Otto, G. Lattice site localization of Zn in InP using the PIXE/channeling technique. *Phys. Status Solidi* **1992**, *132*, 295−304.
(51) Owen, J. The coordination chemistry of nanocrystal surfaces. *Science* **2015**, *347*, 615−616.
(52) Anderson, N. C.; Hendricks, M. P.; Choi, J. J.; Owen, J. S. Ligand Exchange and the Stoichiometry of Metal Chalcogenide Nanocrystals: Spectroscopic Observation of Facile Metal-Carboxylate Displacement and Binding. *J. Am. Chem. Soc.* **2013**, *135*, 18536−18548.
(53) Stein, J. L.; Mader, E. A.; Cossairt, B. M. Luminescent InP Quantum Dots with Tunable Emission by Post-Synthetic Modification with Lewis Acids. *J. Phys. Chem. Lett.* **2016**, *7*, 1315−1320.
(54) Hollingsworth, J. A. Heterostructuring Nanocrystal Quantum Dots Toward Intentional Suppression of Blinking and Auger Recombination. *Chem. Mater.* **2013**, *25*, 1318−1331.
(55) Tschirner, N.; Lange, H.; Schliwa, A.; Biermann, A.; Thomsen, C.; Lambert, K.; Gomes, R.; Hens, Z. Interfacial alloying in CdSe/CdS heteronanocrystals: A Raman spectroscopy analysis. *Chem. Mater.* **2012**, *24*, 311−318.
(56) Baranov, A. V.; Rakovich, Yu. P.; Donegan, J. F.; Perova, T. S.; Moore, R. A.; Talapin, D. V.; Rogach, A. L.; Masumoto, Y.; Nabiev, I. Effect of ZnS shell thickness on the phonon spectra in CdSe quantum dots. *Phys. Rev. B: Condens. Matter Mater. Phys.* **2003**, *68*, 165306.
(57) Shannon, R. t. Revised effective ionic radii and systematic studies of interatomic distances in halides and chalcogenides. *Acta Crystallogr., Sect. A: Cryst. Phys., Diffr., Theor. Gen. Crystallogr.* **1976**, *32*, 751−767.

DOI: 10.1021/acs.chemmater.7b00848
Chem. Mater. 2017, 29, 5192−5199